Atmos. Chem. Phys. Discuss., 13, 18007–18030, 2013
www.atmos-chem-phys-discuss.net/13/18007/2013/
doi:10.5194/acpd-13-18007-2013

Atmospheric Chemistry and Physics Discussions

Turbulent diffusivities and energy dissipation rates in the stratosphere from GOMOS satellite stellar scintillation measurements

N. M. Gavrilov

Saint-Petersburg State University, Atmospheric Physics Department, Russia

Received: 10 June 2013 – Accepted: 22 June 2013 – Published: 5 July 2013

Correspondence to: N. M. Gavrilov (gavrilov@pobox.spbu.ru)

Published by Copernicus Publications on behalf of the European Geosciences Union.

Abstract

Parameters of anisotropic and isotropic spectra of refractivity, density and temperature perturbations obtained from GOMOS satellite measurements of stellar scintillations are used to estimate turbulent Thorpe scales, L_T, diffusivities, K, and energy dissipation rates, ε, in the stratosphere. At low latitudes, average values for altitudes 30–45 km in September–November 2004 are $L_T \sim 1$–1.1 m, $\varepsilon \sim (1.8-2.4)\times10^{-5}$ W kg^{-1}, and $K \sim (1.2-1.6)\times10^{-2}$ m^2 s^{-1} depending on different assumed values of parameters of anisotropic and isotropic spectra. Respective standard deviations of individual values including all kinds of variability are $\delta L_T \sim 0.6$–0.7 m, $\delta\varepsilon \sim (2.3-3.5)\times10^{-5}$ W kg^{-1}, and $\delta K \sim (1.7-2.6)\times10^{-2}$ m^2 s^{-1}. These values correspond to high-resolution balloon measurements of turbulent characteristics in the stratosphere, and to previous satellite stellar scintillation measurements. Distributions of turbulent characteristics at altitudes 30–45 km in low latitudes have maxima at longitudes 30–100° W, 0–60° E and 90–180° E, which correspond to continent locations. Correlations between parameters of anisotropic and isotropic spectra are studied.

1 Introduction

Internal gravity waves (IGWs) propagating upwards are important for dynamical processes and mixing in the middle atmosphere (Fritts and Alexander, 2003). Breaking IGWs may produce turbulent mixing and kinetic energy dissipation and effectively influence the global circulation and composition in the middle atmosphere.

IGW studies use different in situ, ground-based and satellite measurements (Fritts and Alexander, 2003; Wu et al., 2006). Key advantages of satellite measurements are their global exposure. To examine atmospheric mesoscale variations Fetzer and Gille (1994) used satellite data of LIMS (Limb Infrared Monitor of the Stratosphere). Eckermann and Preusse (1999) presented the results of data processing of satellite CRISTA (Cryogenic Infrared Spectrometer and Telescopes for the atmosphere) experiment. Wu

ACPD
13, 18007–18030, 2013

and Waters (1996) and McLandress et al. (2000) studied mesoscale temperature perturbations and obtained their global distribution in the stratosphere and mesosphere from the data of MLS (Microwave Limb Sounder) instrument on board the satellite UARS. Extensive information on atmospheric mesoscale fluctuations were given by GPS/Microlab satellite (Tsuda et al., 2000; Alexander et al., 2002; Gavrilov et al., 2004; Gavrilov and Karpova, 2004). Studies of mesoscale variations using GPS radio occultation technique were continued with satellite CHAMP launched in April 2001 and later with COSMIC group of satellites launched in 2006 (Schmidt et al., 2008; Alexander et al., 2008; Wang and Alexander, 2010).

Recent observations of stellar scintillations with satellites (Gurvich and Kan, 2003a,b; Sofieva et al., 2007, 2009, 2010) provided new information about small-scale perturbations in the stratosphere. Intensity of stellar light going through the atmosphere fluctuate (scintillate), when a satellite observes a star. The amplitude of relative intensity fluctuations may reach hundreds percent (see Sofieva et al., 2010). These scintillations may be due to air temperature and density irregularities produced by IGWs, turbulence and different instabilities, which may produce perturbations of atmospheric refractivity. The smallest scales measurable by the scintillation method may be less than a meter at higher sampling rates of registration. Scintillation measurements may provide information about IGW breaking and turbulence in the stratosphere.

First measurements of stellar scintillations with Russian space stations Salute and Mir provided spectral and statistical characteristics of perturbations (Gurvich et al., 2001), also confirmed the theory of scintillations (Gurvich and Brekhovskikh, 2001). These measurements also allowed determinations of IGW and turbulence spectra characteristics (Gurvich and Kan, 2003a,b; Gurvich and Chunchuzov, 2003).

Multiyear measurements were performed with the Global Ozone Monitoring by Occultation of Stars (GOMOS) instruments from the Envisat satellite (Kyrola et al., 2004). GOMOS contains two photometers recording stellar lights at sampling frequency of 1 kHz synchronously in 473–527 nm and 646–698 nm spectral bands during star sets behind the Earth's limb. These measurements were used to estimate parameters of

ACPD
13, 18007–18030, 2013

anisotropic and isotropic spectra of temperature perturbations produced by IGWs and small-scale turbulence in the stratosphere (Gurvich and Kan, 2003a; Sofieva et al., 2007, 2009, 2010).

In this paper we use these spectra parameters for estimations of turbulent kinetic energy dissipation rates and turbulent diffusivities produced by small-scale isotropic turbulence at altitudes 30–45 km in years 2004 and 2005.

2 Atmospheric perturbation spectra

Sofieva et al. (2007, 2009) estimated scales of isotropic and anisotropic parts of atmospheric perturbation spectra using observations of stellar scintillations with the GOMOS instrument at the Envisat satellite. Scintillations produced by density perturbations along the light pass may give information about small-scale atmospheric dynamics (Tatarskii, 1971). Sofieva et al. (2007, 2009) considered structures of relative fluctuations $v = N_r'/\overline{N_r} \approx -T'/\overline{T}$ of refractivity N_r and temperature T (overbars and primes denote the statistical means and perturbations, respectively). These structures may be described with three-dimensional spectral density $\Phi_v(\boldsymbol{k})$, where $\boldsymbol{k}$ is the wave vector with components (k_x, k_y, k_z) along horizontal axes x, y and vertical axis z respectively. Gurvich and Kan (2003a) and Sofieva et al. (2007) approximated Φ_v with a sum

$$\Phi_v = \Phi_W + \Phi_K, \tag{1}$$

where Φ_W and, Φ_K are statistically independent anisotropic and isotropic components, respectively. The component Φ_W may correspond to anisotropic perturbations, produced, for example, by random IGWs (Smith et al., 1987). Gurvich and Kan (2003a) and Sofieva et al. (2007) approximated this three-dimensional spectrum as

$$\Phi_W(k_a) = C_W \eta^2 \left(k_a^2 + k_0^2\right)^{-5/2} \varphi(k_a/k_W);$$
$$k_a^2 = \eta^2 k_h^2 + k_z^2; \quad k_h^2 = k_x^2 + k_y^2, \tag{2}$$

ACPD
13, 18007–18030, 2013

where C_W and k_0 are constant parameters, η is the anisotropy coefficient, and function $\varphi(k/k_W)$ describes the decay of Φ_W at $k > k_W$. Integration of Eq. (2) gives one-dimensional vertical spectrum $V_W(k_z)$:

$$V_W(k_z) = \int_{-\infty}^{\infty}\int_{-\infty}^{\infty} \Phi_W(k_a)\mathrm{d}k_x\mathrm{d}k_y \approx \frac{2\pi}{3} C_W\left(k_z^2 + k_0^2\right)^{-3/2}. \quad (3)$$

This expression does not depend on the anisotropy coefficient η. At $k_z \gg k_0$ the spectrum Eq. (3) corresponds to k_z^{-3} slope known for saturated IGWs (Smith et al., 1987). As far as $V_W(-k_z) = V_W(k_z)$, one can use symmetric one-dimension spectrum (see Monin and Yaglom, 1975)

$$E_W\left(|k_z|\right) = 2V_W(k_z) = 4\pi C_W\left(k_z^2 + k_0^2\right)^{-3/2}/3. \quad (4)$$

The second component Φ_K in Eq. (1) corresponds to isotropic turbulent irregularities produced by braking IGWs and by other sources. Gurvich and Kan (2003a) and Sofieva et al. (2007) used a theory of locally isotropic turbulence, which gives

$$\Phi_K(k) = 0.033 C_K k^{-11/3} \exp\left[-(k/k_K)^2\right]; \quad k^2 = k_h^2 + k_z^2, \quad (5)$$

where k_K is scale of smallest isotropic perturbations, C_K is the structure characteristic of the random refractivity field (see Monin and Yaglom, 1975). Isotropic one-dimension spectrum $E_K(|k_z|)$ can be obtained by integration of locally isotropic spectrum Φ_K (see Monin and Yaglom, 1975) and at $|k_z| \gg k_K$ has the following form:

$$E_K(|k_z|) \approx 0.25 C_K |k_z|^{-5/3}, \quad (6)$$

which corresponds to the known $-5/3$ power low for Kolmogorov's turbulence (see Monin and Yaglom, 1975). The structure function $D_T(r)$ of locally isotropic temperature field at displacements r (Tatarskii, 1971) have the form

$$D_T(r) = \overline{[T(z+r) - T(z)]^2} = C_T^2 r^{2/3}, \quad (7)$$

ACPD
13, 18007–18030, 2013

where C_T^2 is the structure characteristic of temperature field. According to Monin and Yaglom (1975, § 13.3) for locally isotropic turbulence

$$D_T(r) = 2\int_0^\infty (1 - \cos k'r) E_K(k')\mathrm{d}k' = C_K \bar{T}^2 r^{2/3}. \quad (8)$$

Comparing Eqs. (6) and (7), one can get

$$C_K = C_T^2/\bar{T}^2. \quad (9)$$

Sofieva et al. (2007, 2009) developed algorithms for estimating the four parameters of anisotropic and isotropic spectra Eqs. (2)–(5): the structure characteristics C_K, and C_W and wavenumbers k_W and k_0, which may correspond to inner and outer scales of anisotropic spectrum (Eq. 2). These algorithms were used to obtain these four parameters from observations of stellar scintillations with GOMOS device at the Envisat satellite (Sofieva et al., 2007, 2009).

3 Estimation of turbulence characteristics

In Sect. 3.1 below, we obtain formulae connecting turbulent energy dissipation rates, diffusivities and other turbulent characteristics with parameters of isotropic parts of atmospheric perturbation spectra (Eqs. 4, 5). We use these formulae for estimations of turbulent characteristics in the stratosphere from GOMOS satellite data in Sect. 3.2. Possible correlations between anisotropic and isotropic spectra parameters are considered in Sect. 3.3.

3.1 Relations between turbulent and spectral characteristics

Some theories of turbulent spectra (for example, Lumley, 1964) involve the wavelength, k_t, of crossing one-dimension anisotropic (Eq. 4) and isotropic (Eq. 6) spectra, $E_W(k_t) =$

ACPD
13, 18007–18030, 2013

$E_K(k_t)$, so that

$$k_t \approx (16.8C_W/C_K)^{3/4}. \quad (10)$$

This parameter could be a useful addition to the discussed above parameters of anisotropic (C_W, k_0, k_W) and isotropic (C_K) parts of refractivity perturbation spectra (Eqs. 1–6). Figure 1 shows an example of one-dimension anisotropic (Eq. 4) and isotropic (Eq. 6) components of temperature perturbation spectrum (Eq. 1) and their scales. The wavenumber k_t, as well as k_W, may correspond to edging scale, k_m, between anisotropic perturbations and quasi-isotropic turbulence. An important characteristic of turbulence in stably stratified layers is the Thorpe length $L_T = [\overline{\theta'^2}/(\partial\bar{\theta}/\partial z)^2]^{1/2}$, where θ is potential temperature (see Gavrilov et al., 2005). Contribution to the relative temperature variance produced by turbulent perturbations having $|k_z| \geq k_m$ one may calculate integrating the isotropic spectrum (Eq. 6) as follows:

$$\frac{\overline{T'^2}}{\bar{T}^2} = \int_{k_m}^{\infty} E_K(k')\mathrm{d}k' = 0.37C_K k_m^{-2/3}. \quad (11)$$

Taking account of $\theta'/\bar{\theta} \approx T'/\bar{T}$ (see Tatarskii, 1971) and using (Eq. 11), one can get the following expression for the Thorpe scale:

$$L_{Tm} \approx \frac{g\left(0.37C_K k_m^{-2/3}\right)^{1/2}}{N^2}; \quad N^2 = \frac{g}{\bar{\theta}}\frac{\partial\bar{\theta}}{\partial z}. \quad (12)$$

Similar expression was obtained by Gavrilov et al. (2005). To estimate L_T, one can also use the expression based on the consideration of turbulent energy balance by Ottersten (1969) with hypotheses of incompressibility and isotropic and stationary turbulence (see Gavrilov et al., 2005), which, taking account of (Eqs. 6–8), has the form

$$L_{Te} = \left(0.88C_K g^2\right)^{3/4}/N^3. \quad (13)$$

ACPD
13, 18007–18030, 2013

This formula contains the only one parameter C_K of isotropic perturbation spectrum (Eq. 5). Gavrilov et al. (2005) obtained reasonable agreement between (Eq. 13) and direct measurements of L_T from the data of high-resolution MUTSI balloon measurements in the troposphere and stratosphere. For steady-state turbulence, energy dissipation rate, ε, and turbulent diffusivity, K, are related to the Ozmidov scale, L_O, by

$$\varepsilon \approx L_O^2 N^3; \quad K \approx \beta L_O^2 N, \tag{14}$$

where β is a constant. According to a review by Fukao et al. (1994), β may vary between 0.2 and 1. The frequently used approximation $\beta = Rf/(1-Rf)$, where Rf is the flux Richardson number, often taken as $Rf \approx 0.25$, and giving $\beta \approx 1/3$. Assuming $L_O = cL_T$, Caldwell (1983), and more recently, Galbraith and Kelley (1996), also Fer et al. (2004) proposed the following formulae for estimations of ε and K:

$$\varepsilon \approx (cL_T)^2 N^3; \quad K \approx \beta (cL_T)^2 N. \tag{15}$$

After Gavrilov et al. (2005), considering the result given by Alisse (1999) for stratospheric data, we use $c = 1.15$ and $\beta = 1/3$ below. One may use Eqs. (15) and (10), (12) or (13) for estimations of L_T, ε and K depending on a set of spectral parameters available experimentally. In the case of GOMOS scintillation observations, we have the entire set of parameters C_W, k_0, k_W and C_K, which is enough for usage of any combinations of Equations (10–15). This allows us to compare the results obtained from Eqs. (15) and (10), (12) or (13) in the next section.

3.2 Turbulent diffusivities and energy dissipation rates

The methods of estimating the parameters C_W, k_0, k_W of anisotropic (Eq. 2) and C_K of isotropic (Eq. 5) spectra of atmospheric temperature perturbations from GOMOS satellite observations of star scintillations were described by Sofieva et al. (2007, 2009, 2010). The retrieval uses the standard maximum-likelihood method with a combination

ACPD
13, 18007–18030, 2013

of nonlinear and linear optimization. The authors made nonlinear fits of two parameters k_0 and k_W using the Levenberg–Marquardt algorithm (Press et al., 1992). The parameters C_K and C_W were calculated with the linear weighted least-squares method. Sofieva et al. (2007, 2009, 2010) presented examples of the experimental scintillation spectrums. Usually, experimental scintillations agree with the proposed modeled scintillation spectra, but sometimes peaks, possibly related to quasi-periodic disturbances in the atmosphere, may occur and special filtering of these peaks were applied by Sofieva et al. (2007, 2009, 2010).

In the present paper, we use sets of four parameters C_W, k_0, C_K and k_W from GOMOS scintillation measurements by Sofieva et al. (2007, 2009, 2010) in September–November 2004 at low latitudes between 20° N and 20° S within 3 km thick layers centered at altitudes 30, 35, 40 and 45 km. Also we analyzed the data sets for January 2005 at altitude 30 km and latitudes 34–36° N. For each set of measured parameters C_W and C_K, using Eq. (10), we estimated the wavelength, k_t, of crossing one-dimension anisotropic (Eq. 4) and isotropic (Eq. 5) spectra. The Thorpe scales L_{Tt} and L_{TW} are obtained from Eq. (12) putting $k_m = k_t$ and $k_m = k_W$, respectively, as well as the Thorpe scale L_{Te} from Eq. (13). Then, Eq. (15) gives values of the turbulent energy dissipation rates ε_t, ε_W, ε_e and turbulent diffusivities K_t, K_W, K_e, after substitutions of $L_T = L_{Tt}$, L_{TW}, L_{Te}, respectively. Table 1 gives average values and standard deviations of spectral scales and turbulent characteristics for all used sets of experimental data. Standard deviations shown in Table 1 take into account all variability of individual values, including latitude, longitude and time changes. Standard deviations of the mean values can be obtained dividing corresponding values presented in Table 1 by $\sqrt{n}$, where n is the numbers of values in respective data sets. Figure 2 presents histograms of the spectral parameters and turbulent characteristics for year 2004 at combined altitudes 30–45 km.

For year 2005 Table 1 gives estimations of the average Thorpe scales by different methods $L_T \sim 0.34$–0.44 m at altitude 30 km at middle latitudes in January. Respective average turbulent energy dissipation rates in Table 1 are $\varepsilon \sim (1.8 - 2.9) \times 10^{-6}\,\mathrm{W\,kg^{-1}}$

ACPD
13, 18007–18030, 2013

and turbulent diffusivities $K \sim (1.3-2.0)\times 10^{-3}\,\mathrm{m^2\,s^{-1}}$. Differences in these estimations are caused by usage of different $k_m = k_t$ and $k_m = k_W$ in Eq. (12) for calculation of L_{Tt} and L_{TW} and usage of Eq. (13) to calculate L_{Te}, also by possible uncertainties in semiempirical coefficients in these formulae. Clayson and Kantha (2008) estimated turbulent characteristics in year 2005 at middle latitudes 30–39° N and longitudes 84–104° W from high-resolution radiosonde data. At altitudes about 25 km they found average values of $L_T < 1$ m, $\varepsilon \sim 10^{-6} - 10^{-5}\,\mathrm{W\,kg^{-1}}$ and $K < 10^{-2}\,\mathrm{m^2\,s^{-1}}$, which are consistent with average turbulent characteristics for year 2005 presented in Table 1.

Consideration of Table 1 for year 2004 shows monotonic decrease in stability and average N^2 values from altitude 30 km to 45 km at low latitudes. Average characteristic wavelengths k_0 and k_W of the anisotropic spectrum (Eq. 2) are also decreasing with height in Table 1, while parameters C_W and C_K in Eqs. (2) and (5) have maxima at altitude 40 km. Estimated average wavelengths of crossing one-dimensional anisotropic (Eq. 4) and isotropic (Eq. 6) spectra k_t in Table 1 are generally larger than the wavelength of anisotropic spectra decrease k_W (see Fig. 1). Estimates of Thorpe scales L_{TW} and L_{Te} averaged over altitudes 30–45 km are quite close in Table 1, while average L_{Tt} is little bit smaller. At particular altitudes in Table 1 differences between L_{Tt}, L_{TW} and L_{Te} are larger and may be partly caused by uncertainties in semi-empirical constants in Eqs. (12) and (13). Relative differences between maximum and minimum values ε_t, ε_W, ε_e do not exceed 30–50 % at different altitudes in Table 1 and respective K_t, K_W, K_e do not differ more than 20–40 %.

Figure 3 shows latitude-longitude distributions of different estimates of turbulent energy dissipation rates in September–November 2004 averaged over altitudes 30–45 km. One can see very similar distributions of all estimates $\varepsilon_t, \varepsilon_W$ and ε_e. This show that all expressions (Eq. 12) with $k_m = k_t$ and $k_m = k_W$, and (Eq. 13) may be used for estimations of Thorpe scales and subsequent estimations of turbulent energy dissipation rates and turbulent diffusivities (Eq. 15), depending on spectra parameters available from experiments. Gurvich et al. (2007) presented similar distributions of struc-

ACPD
13, 18007–18030, 2013

ture characteristic of temperature field obtained from GOMOS observations for July–September 2003 at altitude 42 km.

Figure 4 shows latitude-longitude distributions of turbulent diffusivity estimate K_W in September–November 2004 at different altitudes. One can see substantial variability of these distributions in altitude. Latitude–longitude distributions similar to Fig. 4 were obtained for C_K and other estimates of turbulent diffusivity and turbulent energy dissipation rate. Although maxima of K_W are concentrated at the same longitudes as C_K maxima in Fig. 3, their distributions may vary at different altitudes in Fig. 4.

3.3 Correlations between spectra parameters

Parameters C_W, k_0, k_W of anisotropic (Eq. 2) and C_K of isotropic (Eq. 5) spectra may be related to each other. For example, increasing small-scale isotropic turbulence may cause increased dissipation of larger scale anisotropic motions in the atmosphere, also instabilities of anisotropic motions may cause generation of increased isotropic turbulence. At numbers of registered values $n > 580$ at different altitudes in year 2004 in Table 1, the hypothesis about nonzero linear dependence between two variables has confidence > 0.999, when the absolute values of cross-correlation coefficients between them are $|r| > 0.1$ (see Press et al., 1992). Table 2 shows cases, when $|r|$ were larger 0.1 and r had the same signs at all altitudes for data sets presented in Table 1. One can see that the largest positive correlations exist between parameters C_W and C_K. Smaller positive correlations may exist between C_W and k_0 and negative correlation between C_W and k_W in Table 2.

Figure 5 shows scatter plots for pairs of spectra parameters presented in Table 2 for year 2004 within the entire altitude range 30–45 km. Dependences between these parameters in Fig. 5 can be approximated with power laws $y = aC_W^\gamma$, where y may represent any of quantities C_K, k_0, or k_W. Corresponding power law parameters a and γ for these quantities, obtained with least-square fitting at different altitudes, are given in Table 2.

ACPD
13, 18007–18030, 2013

4 Discussion

Average values of Thorpe scales L_{Ti} are about, or smaller than 1 m in Table 1 at altitudes 30–35 km. Respective average turbulent energy dissipation rates $\varepsilon_i \leq 2 \times 10^{-5}$ W kg^{-1} and turbulent diffusivities $K_i \leq 1.3 \times 10^{-2}$ m^2 s^{-1}. Gavrilov et al. (2005) obtained the same orders of magnitude for these quantities from the analysis of high-resolution temperature profiles obtained during the MUTSI campaign. High-resolution radio sound measurements by Clayson and Kantha (2008) also gave average values of L_T, ε, and K, which are consistent with average turbulent characteristics for year 2005 presented in Table 1 (see above).

Gurvich and Chunchuzov (2003b) estimated parameters of anisotropic (Eq. 2) and isotropic (Eq. 5) spectra at altitudes 25–70 km from measurements of stellar scintillations performed on board the space stations Mir and Salyut. They found systematic decrease in average k_W from 0.5 to 0.1 m^{-1} and increase in C_K from 10^{-9} to 10^{-8} m$^{-2/3}$, when altitude changed from 30 to 50 km. This is generally consistent with behavior of k_W and C_K at different altitudes between 30 and 45 km in Table 1 in year 2004. Parameter of anisotropic spectrum C_W obtained by Gurvich and Chunchuzov (2003) is less variable in height and $C_W \sim (5-7) \times 10^{-11}$ m^{-2} with a maximum at altitudes about 40 km, which is similar to C_W behavior in Table 1. Gurvich and Kan (2003) estimated turbulent kinetic energy dissipation rates using k_W obtained from the space stations Salyut and Mir. Their average ε increased with height from 10^{-6} to 5×10^{-5} W kg^{-1} between altitudes 30 and 50 km. Values ε_i in Table 1 generally correspond to this behavior. Differences in exact values of mentioned parameters and characteristics in Table 1 and those estimated by Gurvich and Chunchuzov (2003) and Gurvich and Kan (2003b) may be caused by differences in years, seasons and latitudes of observations with GOMOS and the space stations Salyut and Mir.

One of sources of turbulence in the middle atmosphere could be breaking IGWs (Lindzen, 1981; Fritts and Alexander, 2003). This may explain observed in Table 2 and in Fig. 5 positive correlation between parameters C_W and C_K. It is usually sup-

ACPD
13, 18007–18030, 2013

posed that anisotropic spectra (Eqs. 2 and 3) are mainly composed of saturated IGWs (Fritts and Alexander, 2003; Sofieva et al., 2007, 2010). Larger C_W may cause more intensive breaking of these IGWs and may produce larger amplitudes C_K of isotropic spectra of small-scale turbulence. Increased turbulence generated by stronger IGWs may produce stronger dissipation of shorter waves and decrease the cutoff wavelength of anisotropic spectrum k_W (see negative correlation between C_W and k_W in Table 2).

In Fig. 3, distributions of C_K and ε_i at altitudes 30–45 km in low latitudes have maxima at longitudes corresponding to locations of America, Africa and South-East Asia (see Sect. 3.2). Maxima of IGW intensity and potential energy at similar longitudes at altitudes 15–25 km in the stratosphere were obtained with low-orbit GPS satellite measurements (Gavrilov, 2007; Alexander et al., 2008; Wang and Alexander, 2010). This may confirm the hypothesis about turbulence generation by breaking IGWs. Variability of latitude-longitude distributions of turbulent characteristics in Fig. 4 may show that interactions between anisotropic IGWs and isotropic turbulent spectra may be more complicated than simple model of saturated monochromatic IGWs (Lindzen, 1981). For example, breaking of long-wave IGW may produce intensive turbulence, which can suppress amplitudes of shorter-wave spectral components. Therefore, above intensive turbulent zones, spectra of upward propagating IGWs may become weaker, then those spectra above laminar layers, which can become unstable and generate turbulence there. Such interactions between IGW and turbulent spectra may produce interspersed locations of intensive IGWs and turbulence at different altitudes.

In this paper, we used three estimates of the Thorpe scales from Eqs. (10), (12) and (13), namely $L_T = L_{Tt}$, L_{TW}, L_{Te}, and respective values of turbulent energy dissipation rates ε_t, ε_W, ε_e and turbulent diffusivities K_t, K_W, K_e. These estimates utilize different sets of spectra parameters: C_W, C_K for L_{Tt}; C_K, k_W for L_{TW}, and just C_K for L_{Te}. Table 1 shows that L_{Tt}, ε_t, K_t are usually smaller than respective L_{TW}, ε_W, K_W. This is the result of generally larger wavenumbers k_t of crossing anisotropic and isotropic spectra compared to k_W (see Fig. 1). As was mentioned in Sect. 3.2, differences between considered estimates of turbulent characteristics are usually not large, and one can

ACPD
13, 18007–18030, 2013

use any of these estimates depending on available sets of anisotropic and isotropic spectra scales.

5 Conclusions

In this paper, we use parameters of spectra of anisotropic and isotropic refractivity, density and temperature perturbations obtained from GOMOS satellite measurements of stellar scintillations to estimate turbulent Thorpe scales, L_T, diffusivities, K, and energy dissipation rates, ε, in the stratosphere. At low latitudes, average values for altitudes 30–45 km in September–November 2004 are $L_T \sim 1$–1.1 m, $\varepsilon \sim (1.8-2.4)\times 10^{-5}\,\mathrm{W\,kg^{-1}}$, and $K \sim (1.2-1.6)\times 10^{-2}\,\mathrm{m^2\,s^{-1}}$ depending on different sets of used parameters. Respective standard deviations due to all kinds of individual values variability are $\delta L_T \sim 0.6$–0.7 m, $\delta\varepsilon \sim (2.3-3.5)\times 10^{-5}\,\mathrm{W\,kg^{-1}}$, and $\delta K \sim (1.7-2.6)\times 10^{-2}\,\mathrm{m^2\,s^{-1}}$. These values correspond to high-resolution balloon measurements of turbulent characteristics in the stratosphere, and to previous satellite stellar scintillation measurements. At latitudes 20° S–20° N, distributions of turbulent characteristics have maxima at longitudes 30–100° W, 0–60° E and 90–180° E, which correspond to location of continents. Largest positive correlations exist between parameters C_W and C_K. Smaller positive correlations may exist between C_W and k_0, also negative correlation between C_W and k_W.

Acknowledgements. This work was partly supported by the Russian Basic Research Foundation. The author thanks Victoria F. Sofieva for providing databases of parameters of anisotropic and isotropic temperature perturbation spectra from GOMOS satellite measurements and for useful discussions.

References

Alexander, M. J., Tsuda, T., and Vincent, R. A.: Latitudinal variations observed in gravity waves with short vertical wavelengths, J. Atmos. Sci., 59, 1394–1404, 2002.

ACPD
13, 18007–18030, 2013

Alexander, S. P., Tsuda, T., Kawatani, Y., and Takahashi, M.: Global distribution of atmospheric waves in the equatorial upper troposphere and lower stratosphere: COSMIC observations of wave mean flow interactions, J. Geophys. Res., 113, D24115, doi:10.1029/2008JD010039, 2008.

Alisse, J. R.: Turbulence en atmosphere stable, Une etude quantitative, These de doctorat, Univ. Paris VI, 1999.

Caldwell, D. R.: Oceanic turbulence: big bangs or continuous creation?, J. Geophys. Res., 88, 7543–7550, 1983.

Clayson, C. A. and Kantha, L.: On turbulence and mixing in the free atmosphere inferred from high-resolution soundings, J. Atmos. Oceanic. Technol., 25, 833–851, 2008.

Eckermann, S. and Preusse, P.: Global measurements of stratospheric mountain waves from space, Science, 286, 1534–1537, 1999.

Fer, I., Skogseth, R., and Haugan, P. M.: Mixing of the Storjorden overflow (Svalbard Archipelago) inferred from density overturns, J. Geophys. Res., 109, 1–14, 2004.

Fetzer, E. J. and Gille, J. C.: Gravity wave variance in LIMS temperatures. Part I: Variability and comparison with background winds, J. Atmos. Sci., 51, 2461–2483, 1994.

Fritts, D. C. and Alexander, M. J.: Gravity wave dynamics and effects in the middle atmosphere, Rev. Geophys. 41, 1, doi:10.1029/2001RG000106, 2003.

Fukao, S., Yamanaka, M. D., Ao, N., Hocking, W. K., Sato, T., Yamamoto, M., Nakamura, T., Tsuda, T., and Kato, S.: Seasonal variability of vertical eddy diffusivity in the middle atmosphere, 1. Three-year observations by the middle and upper atmosphere radar, J. Geophys. Res., 99, 18973–18987, 1994.

Galbraith, P. S. and Kelley, D. E.: Identifying overturns in CTD profiles, J. Atmos. Ocean. Technol., 13, 688–702, 1996.

Gavrilov, N. M.: Structure of the mesoscale variability of the troposphere and stratosphere found from radio refraction measurements via CHAMP satellite, Izv. Atmos. Ocean. Phy.+, 43, 451–460, 2007.

Gavrilov, N. M. and Karpova, N. V.: Global structure of mesoscale variability of the atmosphere from satellite measurements of radio wave refraction, Izv. Atmos. Ocean. Phy.+, 40, 747–758, 2004.

Gavrilov, N. M., Karpova, N. V., Jacobi, Ch, Gavrilov, A. N.: Morphology of atmospheric refraction index variations at different altitudes from GPS/MET satellite observations, J. Atmos. Solar-Terr. Phys., 66, 427–435, 2004.

ACPD
13, 18007–18030, 2013

Gavrilov, N. M., Luce, H., Crochet, M., Dalaudier, F., and Fukao, S.: Turbulence parameter estimations from high-resolution balloon temperature measurements of the MUTSI-2000 campaign, Ann. Geophys., 23, 2401–2413, doi:10.5194/angeo-23-2401-2005, 2005.

Gurvich, A. S. and Brekhovskikh, V. L.: Study of the turbulence and inner waves in the stratosphere based on the observations of stellar scintillations from space: a model of scintillation spectra, Wave. Random Media, 11, 163–181, 2001.

Gurvich, A. S. and Chunchuzov, I. P.: Parameters of the fine density structure in the stratosphere obtained from spacecraft observations of stellar scintillations, J. Geophys. Res., 108, 4166, doi:10.1029/2002JD002281, 2003.

Gurvich, A. S. and Kan, V.: Structure of air density irregularities in the stratosphere from spacecraft observations of stellar scintillation: 1. Three-dimensional spectrum model and recovery of its parameters, Izvestia, Atmos. Ocean. Phys., 39, 300–310, 2003a.

Gurvich, A. S. and Kan, V.: Structure of air density irregularities in the stratosphere from spacecraft observations of stellar scintillation: 2. Characteristic scales, structure characteristics, and kinetic energy dissipation, Izvestiya, Atmos. Ocean. Phys., 39, 311–321, 2003b.

Gurvich, A. S., Kan, V., Savchenko, S. A., Pakhomov, A. I., and Padalka, G. I.: Studying the turbulence and internal waves in the stratosphere from spacecraft observations of stellar scintillation: I I. Probability distributions and scintillation spectra, Izvestia, Atmos. Ocean. Phys., 37, 452–465, 2001.

Kyrola, E., Tamminen, J., Leppelmeier, G. W., Sofieva, V., Hassinen, S., Bertaux, J. L., Hauchecorne, A., Dalaudier, F., Cot, C., Korablev, O., Fanton d'Andon, O., Barrot, G., Mangin, A., Théodore, B., Guirlet, M., Etanchaud, F., Snoeij, P., Koopman, R., Saavedra, L., Fraisse, R. Fussen, D., and Vanhellemont, F.: GOMOS on Envisat: an overview, Adv. Space Res., 33, 1020–1028, doi:10.1016/S0273-1177(03)00590-8, 2004.

Lumley, J. L.: The spectrum of nearly inertial turbulence in a stably stratified fluid, J. Atmos. Sci., 21, 99–102, 1964.

Lindzen, R. S.: Turbulence and stress owing to gravity wave and tidal breakdown, J. Geophys. Res., 86, 9707–9714, 1981.

McLandress, C., Alexander, M. J., and Wu, D.: Microwave limb sounder observations of gravity waves in the stratosphere: a climatology and interpretation, J. Geophys. Res., 105, 11947–11967, 2000.

Monin, A. S. and Yaglom, A. M.: Statistical Fluid Mechanics, vol. 2, MIT Press, Cambridge, Mass, 1975.

ACPD
13, 18007–18030, 2013

Press, W. H., Teukolsky, S. A., Vetterling, W. T., and Flannery, B. P.: Numerical Recipes in FORTRAN, The Art of Scientific Computing, Oxford, Clarendon, 1992.
Smith, S. A., Fritts, D. C., and VanZandt, T. E.: Evidence of a saturation spectrum of atmospheric gravity waves, J. Atmos. Sci., 44, 1404–1410, 1987.
Sofieva, V. F., Gurvich, A. S., Dalaudier, F., and Kan, V.: Reconstruction of internal gravity wave and turbulence parameters in the stratosphere using GOMOS scintillation measurements, J. Geophys. Res., 112, D12113, doi:10.1029/2006JD007483, 2007.
Sofieva, V. F., Gurvich, A. S., and Dalaudier, F.: Gravity wave spectra parameters in 2003 retrieved from stellar scintillation measurements by GOMOS, Geophys. Res. Lett., 36, L05811, doi:10.1029/2008GL036726, 2009.
Sofieva, V. F., Gurvich, A. S., and Dalaudier, F.: Mapping gravity waves and turbulence in the stratosphere using satellite measurements of stellar scintillation, Phys. Scripta T, 142, 014043, doi:10.1088/0031-8949/2010/T142/014043, 2010.
Schmidt, T., de la Torre, A., and Wickert, J.: Global gravity wave activity in the tropopause region from CHAMP radio occultation data, Geophys. Res. Lett., 35, L16807, doi:10.1029/2008GL034986, 2008.
Tatarskii, V. I.: The Effects of the Turbulent Atmosphere on Wave Propagation, US Dep. of Commer., Washington, D.C., 1971.
Tsuda, T., Nishida, M., Rocken, C., and Ware, R. H.: A global morphology of gravity wave activity in the stratosphere revealed by the GPS occultation data (GPS/MET), J. Geophys. Res., 105, 7257–7274, 2000.
Wang, L. and Alexander, M. J.: Global estimates of gravity wave parameters from GPS radio occultation temperature data, J. Geophys. Res., 115, D21122, doi:10.1029/2010JD013860, 2010.
Wu, D. and Waters, J.: Gravity-wave-scale temperature fluctuations seen by the UARS MLS, Geophys. Res. Lett., 23, 3289–3292, 1996.
Wu, D. L., Preusse, P., Eckermann, S. D., Jiang, J. H., de la Torre, J. M., Coy, L., Lawrence, B., and Wang, D. Y.: Remote sounding of atmospheric gravity waves with satellite limb and nadir techniques, Adv. Space Res., 37, 2269–2277, doi:10.1016/j.asr.2005.07.031, 2006.

ACPD
13, 18007–18030, 2013

Table 1. Averages and standard deviations of the spectra parameters and turbulence characteristics.

Year	2004	2004	2004	2004	2004	2005
Months	9–11	9–11	9–11	9–11	9–11	1
z, km	30	35	40	45	30÷ 45	30
Latitudes	−20 ÷ 20	−20 ÷ 20	−20 ÷ 20	−20 ÷ 20	−20 ÷ 20	34 ÷ 36
n	594	596	597	587	2374	147
N^2, 10^{-4} s^{-1}	5.13 ± 0.29	5.11 ± 0.51	5.01 ± 0.38	4.36 ± 0.37	4.80 ± 0.51	4.94 ± 0.48
C_W, 10^{-11} m^{-2}	3.78 ± 1.08	4.26 ± 1.63	5.71 ± 2.55	4.51 ± 2.42	4.57 ± 2.19	4.52 ± 1.39
k_0, 10^{-3} m^{-1}	4.02 ± 3.31	3.43 ± 3.25	2.75 ± 3.30	1.77 ± 1.99	2.99 ± 3.13	5.34 ± 3.32
C_K, 10^{-9} m$^{-2/3}$	1.36 ± 0.74	3.37 ± 1.55	5.72 ± 3.68	3.02 ± 2.65	3.37 ± 2.91	0.80 ± 0.32
k_W, m^{-1}	0.41 ± 0.09	0.34 ± 0.10	0.22 ± 0.08	0.13 ± 0.06	0.27 ± 0.14	0.47 ± 0.09
k_t, m^{-1}	0.62 ± 0.19	0.34 ± 0.12	0.34 ± 0.20	0.48 ± 0.28	0.44 ± 0.23	1.04 ± 0.30
L_{Tt}, m	0.51 ± 0.19	1.00 ± 0.35	1.37 ± 0.66	1.01 ± 0.59	0.98 ± 0.58	0.34 ± 0.10
L_{TW}, m	0.57 ± 0.15	0.98 ± 0.26	1.47 ± 0.55	1.41 ± 0.63	1.11 ± 0.59	0.44 ± 0.11
L_{Te}, m	0.53 ± 0.20	1.07 ± 0.42	1.60 ± 0.82	1.19 ± 0.75	1.10 ± 0.72	0.38 ± 0.13
ε_t, 10^{-5} W kg^{-1}	0.46 ± 0.46	1.66 ± 1.10	3.37 ± 3.11	1.64 ± 2.24	1.78 ± 2.32	0.18 ± 0.10
ε_W, 10^{-5} W kg^{-1}	0.53 ± 0.30	1.52 ± 0.74	3.58 ± 2.62	2.83 ± 3.72	2.11 ± 2.90	0.29 ± 0.13
ε_e, 10^{-5} W kg^{-1}	0.49 ± 0.48	1.92 ± 1.46	4.66 ± 4.45	2.33 ± 3.81	2.35 ± 3.54	0.23 ± 0.14
K_t, 10^{-2} m^2 s^{-1}	0.30 ± 0.30	1.10 ± 0.78	2.28 ± 2.12	1.26 ± 1.75	1.24 ± 1.65	0.13 ± 0.07
K_W, 10^{-2} m^2 s^{-1}	0.34 ± 0.20	1.01 ± 0.52	2.42 ± 1.81	2.18 ± 2.99	1.49 ± 2.24	0.20 ± 0.09
K_e, 10^{-2} m^2 s^{-1}	0.32 ± 0.32	1.29 ± 1.08	3.16 ± 3.08	1.79 ± 3.06	1.64 ± 2.62	0.16 ± 0.10

ACPD
13, 18007–18030, 2013

Table 2. Cross-correlation coefficients r and parameters of power dependences between parameters of anisotropic and isotropic components of atmospheric perturbation spectra.

Year	2004	2004	2004	2004	2004	2005
Months	9–11	9–11	9–11	9–11	9–11	1
z, km	30	35	40	45	30÷ 45	30
Latitudes	−20 ÷ 20	−20 ÷ 20	−20 ÷ 20	−20 ÷ 20	−20 ÷ 20	34 ÷ 36
n	594	596	597	587	2374	147
C_W, 10^{-11} m^{-2}	3–8	3–8	2–9	2–9	2–11	2–8
			$C_K \sim a(C_W)^\gamma$			
r	0.24	0.37	0.32	0.36	0.44	0.49
a	2.05×10^{-4}	5.17×10^{-4}	48.7	0.068	55.1	0.69
γ	0.47	0.50	0.97	0.72	1.00	0.87
			$k_0 \sim a(C_W)^\gamma$			
r		0.13	0.33	0.38	0.15	
a		50.0	1.10×10^6	61.6	0.39	
γ		0.42	0.85	0.45	0.22	
			$k_W \sim a(C_W)^\gamma$			
r	−0.36		−0.20	−0.20	−0.25	−0.45
a	8.12		7.48×10^{-3}	5.18×10^{-3}	1.26×10^{-4}	1.74×10^{-3}
γ	−0.35		−0.14	−0.13	−0.32	−0.23

ACPD
13, 18007–18030, 2013

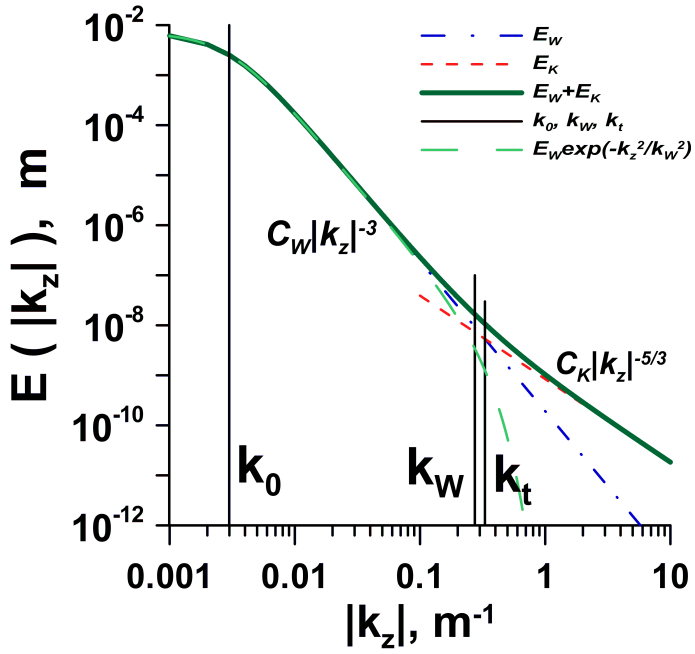

Fig. 1. One-dimension anisotropic (Eq. 4) and isotropic (Eq. 6) components of temperature perturbation spectrum (Eq. 1) for average parameters at altitudes 30–45 km given in Table 1.

ACPD
13, 18007–18030, 2013

Turbulent diffusivities and energy dissipation rates in the stratosphere

N. M. Gavrilov

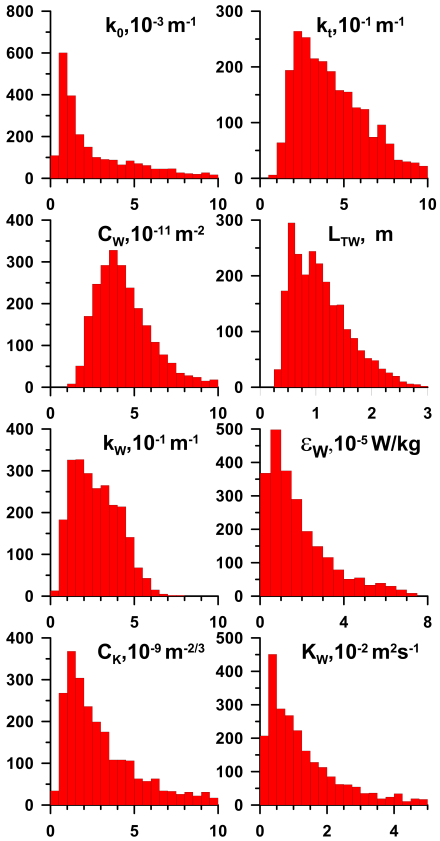

Fig. 2. Histograms of anisotropic and isotropic spectra parameters and turbulent characteristics in year 2004 at altitudes 30–45 km.

ACPD
13, 18007–18030, 2013

Turbulent diffusivities and energy dissipation rates in the stratosphere

N. M. Gavrilov

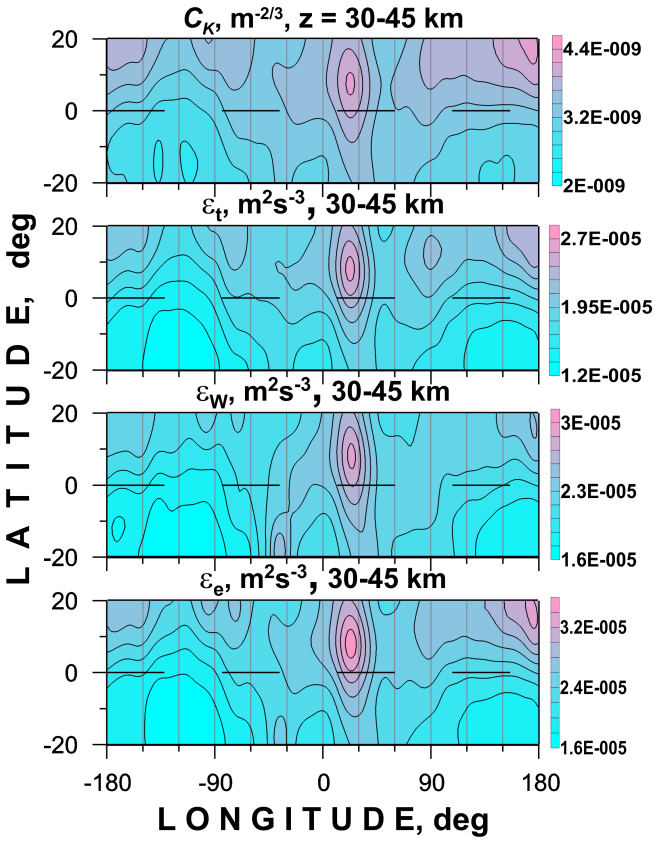

Fig. 3. Latitude-longitude distributions of different estimates of turbulent energy dissipation rates in September–November 2004 at altitudes 30–45 km.

ACPD
13, 18007–18030, 2013

Turbulent diffusivities and energy dissipation rates in the stratosphere

N. M. Gavrilov

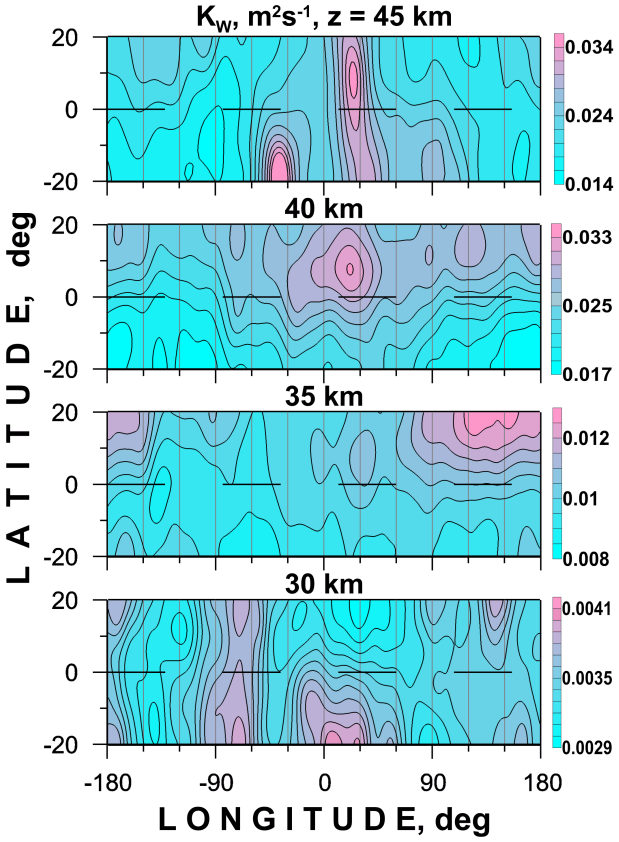

Fig. 4. Latitude-longitude distributions of turbulent diffusivity estimate K_W in September–November 2004 at different altitudes.

ACPD
13, 18007–18030, 2013

Turbulent diffusivities and energy dissipation rates in the stratosphere

N. M. Gavrilov

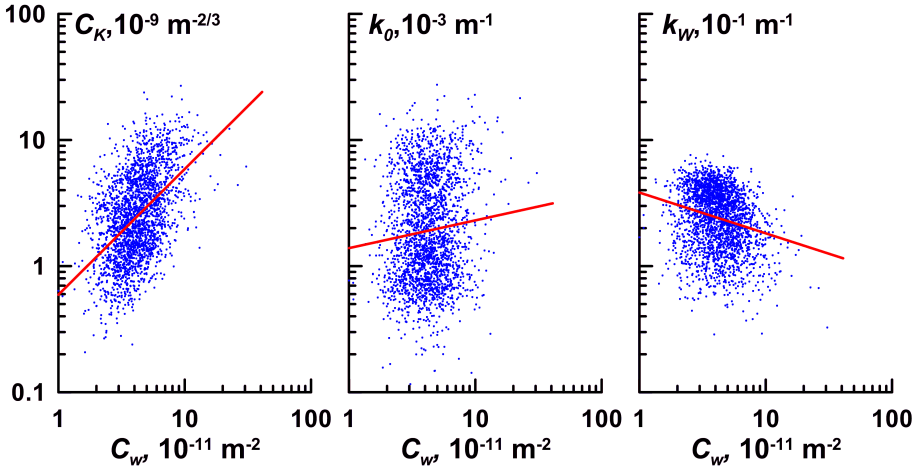

Fig. 5. Scatter plots for the spectra parameter pairs presented in Table 2 for year 2004 at altitudes 30–45 km.

ACPD
13, 18007–18030, 2013